International Journal of Applied Engineering Research ISSN 0973-4562 Volume 12, Number 12 (2017) pp. 3015-3022

Integrated Mathematical Model and Control Design for Hybrid Active Power Filter

VanBao Chau[1]

Faculty of Electrical & Electronic Engineering - Ho Chi Minh City University of Transport, Ho Chi Minh City, 700000, Viet Nam.

CongPhuong Vo[2]

Faculty of Electrical & Electronic Engineering - Ho Chi Minh City University of Transport, Ho Chi Minh City, 700000, Viet Nam.

Minh Thuyen Chau[3,*]

Faculty of Electrical Engineering, Industrial University of Ho Chi Minh City, Ho Chi Minh City, 700000, Viet Nam.

[3]***ORCID: 0000-0002-2565-3513, Scopus Author ID: 49361058500***

Abstract

In this paper, an integrated mathematical model of Hybrid Active Power Filter (HAPF) under two types of closed loop control methods is proposed based on the analysis of operating principle. A new control method of HAPF is presented based on integrated mathematical model. It is a combination of the Hysteresis and Adaptive Fuzzy-Neural controllers. The Adaptive Fuzzy Neural controller aims to identify nonlinear processes of HAPF and predict a new output value. This output value is used to minimize error between the reference and predicted output values. So, the parameters of the Adaptive Fuzzy-Neural controller will be online adjusted based on cost function minimum criteria. The Hysteresis controller is used to further reduce dynamic response time and contribute minimum error in steady-state. For this reason, the proposed control method has advantages of both Hysteresis controller and Adaptive Fuzzy-Neural controller. To prove stability of control method, a stable analysis based on Lyapunov theorem is implemented. And to demonstrate effectiveness and robustness of the proposed control method, simulation results are performed in three cases: the parameters of the system are not changed, the parameters of the system are changed and the grid voltage is unbalanced. Compared to the traditional Hysteresis and fuzzy-neural controllers, simulation results demonstrated that the proposed control method has the shorter dynamic response time, capability to cancel harmonics is better and especially the ability to adapt to the changes of the system is very well.

Keywords: Hybrid Active Power Filter, Fuzzy Neural controller, Hysteresis controller, Predictive control, Mathematical model.

INTRODUCTION

The presence of harmonic components in the power system is a cause of the problems such as: increase losses, voltage distortion, overheating, overloading, etc. So, to cancel harmonic problems we often use Passive Power Filters (PPFs) [1-3]. The PPFs have simple structure, and is inexpensive, but it also has several disadvantages due to resonance, sensitive to environments, compensation characteristic is often influenced by the source impedance, effective in improving harmonic distortion is poor and not flexible. In order to improve the PPF's disadvantages, the Active Power Filter (APF) [4-6] appears in 1970s. It is often shunted with nonlinear load to eliminate harmonic currents and reactive power compensation, which has the capability of online compensation cling to harmonic currents of non-linear load. The APF does not cause symptoms consonance with the impedance of the grid. However, APF also exits many disadvantages as high cost, low capacity and is difficult to use in high voltage grids. Another topology was expanded to exterminate harmonics, namely Hybrid Active Power Filter (HAPF) [7-8]. The HAPF topology is the combination of the APF and PPF_s. Therefore, it has the advantages of both PPF and APF. The purpose of HAPF development is to decrease

APF duty. For this reason, the HAPF can be used in high voltage and capacity grids. It has achieved high performance in reducing harmonics and reactive power compensation with a low capacity of APF.

Nevertheless, the operating effectiveness of HAPF is dependent on the control strategy and control method. The control strategies have been used for HAPF are: control strategy based on source harmonic current and load harmonic current. However, there is no analysis to compare between two above control strategies. The control methods that have been used for HAPF can be summarized following as: the control method using conventional PI, Hysteresis, single-Fuzzy logic, Neural Network controllers. The outstanding points of the control method using Hysteresis controller [9] are simple and fast response but its disadvantages depend on switching frequency and received the result is not good. The control method using a conventional PI controller [10] is achieved result is poor, large steady-state error and especially when the load changes in large-scale then this controller proves inefficient, steady-state error will be very large and can be instability. Although, the conventional PI controller has the advantages of simple mathematical model and easy implementation. The advantages of using the single-fuzzy logic controller are easy to define, high flexibility and acceptable result. However, we rarely used only alone a single-fuzzy logic controller to control because its input-output membership functions are fixed during the control process, therefore it is very difficult to achieve a result minimum steady-state error, so in the process of controlling this controller is usually combined with conventional controller [11-13] to improve its working capacity. If the controller uses neural network [14-20] then the result gives dynamic response is relatively slow or transient time is large, because the achieved result is depend on the training process and the input and output relations is very difficult to express. However, the controller using neural network also shows many advantages such as: self-learning ability, identity and self-adaptive. These points are very convenient for nonlinear controls. So, this paper implements an integrated mathematical model of HAPF and proposes a new control method for HAPF. This method has many advantages such as: minimum error, decrease dynamic response time and especially the ability to adapt to the changes of the system is very well.

This paper is structured as follows: section 1 gives the introduction of the achieved researches on HAPF. The integrated mathematical model of HAPF is highlighted in section 2. Section 3 introduces the proposed control method for HAPF. Stability analysis of the proposed control method is presented in section 4. Simulation results are presented in section 5. Finally, conclusions are drawn in section 6.

INTEGRATED MATHEMATICAL MODEL OF HAPF

The structure of a HAPF [10] is shown as in Figure 1.

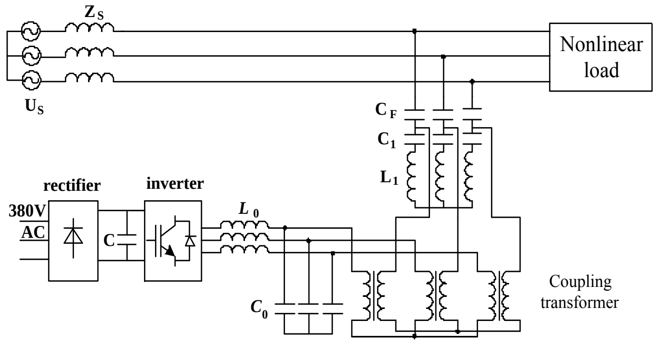

Figure 1. Structure of HAPF

Where: U_s and Z_s are the voltage and impedance of the grid, L_0 and C_0 are the inductor and capacitor of the output filter, C_F is the injection capacitor, L_1 and C_1 are the inductor and capacitor tune at the fundamental frequency and then compose with the injection capacitor C_F to further decrease the power of APF.

Single-phase equivalent circuit of the HAPF is shown in Figure 2.

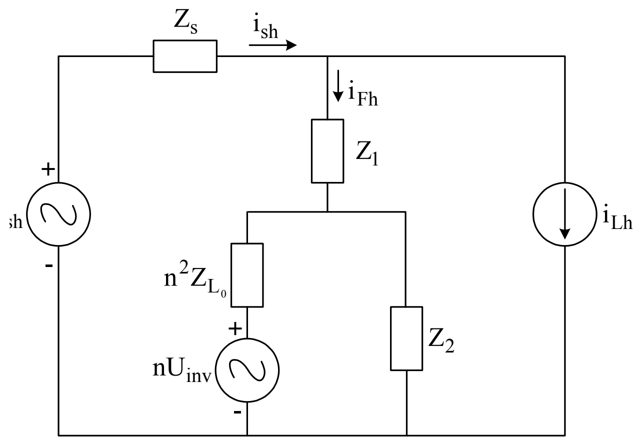

Figure 2. Single-phase equivalent circuit in the domain of harmonic of HAPF

Trong đó: Z_1, Z_2 và Z_{L0} are the impedance of injection capacitor, impedance between the fundamental resonance circuit and capacitor and impedance of the output filter inductor, respectively.

According to [10], the inverter in HAPF is controlled as a current controlled voltage source. There are two types of closed-loop control methods will be discussed as follows:

1) The first closed loop control method is shown as Figure 3.

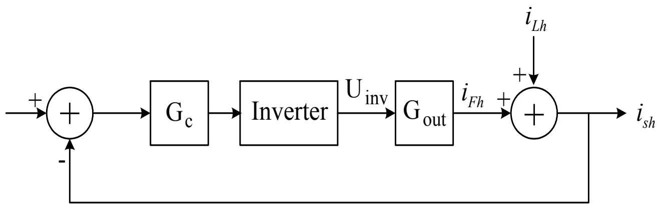

Figure 3. First closed loop control method of HAPF

According to Fig. 3, we have:

$$U_{inv} = G_c(s).G_{inv}(s).(-i_{sh}) \quad (1)$$

$$K_1(s) = -G_c(s).G_{inv}(s) \quad (2)$$

$$U_{inv} = K_1(s).i_{sh} \quad (3)$$

2) The second closed loop control method is shown as Figure 4.

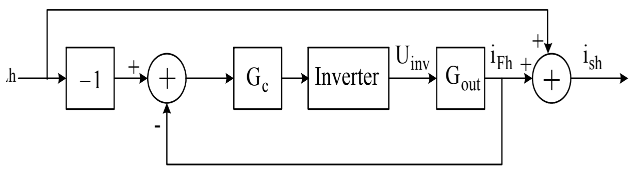

Figure 4. Second closed loop control method of HAPF

According to Fig. 4, we have:

$$U_{inv} = -\frac{G_c(s).G_{inv}(s)}{1+G_c(s).G_{inv}(s).G_{out}(s)}.i_{Lh} \quad (4)$$

$$K_2(s) = -\frac{G_c(s).G_{inv}(s)}{1+G_c(s).G_{inv}(s).G_{out}(s)} \quad (5)$$

$$U_{inv} = K_2(s).i_{Lh} \quad (6)$$

Where: G_c is the transfer function of the controller and G_{out} is the transfer function of compensation harmonic currents i_{Fh} to inverter output voltage U_{inv} and presented in Eq. (7):

$$G_{out}(s) = \frac{i_{Fh}}{U_{inv}} = \frac{nZ_2}{Z_2(Z_1+Z_S)+n^2 Z_{L0}(Z_1+Z_2+Z_S)} \quad (7)$$

The reverse of load harmonic current is regarded as the reference signal, and the output harmonic current of HAPF injected into the grid is regarded as the feedback signal.

From Figure 3 and Figure 4, we can see that: the transfer function of the grid harmonic currents to the load harmonic currents are the same and can be obtained by equations (8). It means that the effectiveness and characteristics of HAPF under the two types of closed loop control methods are exactly the same.

$$\frac{i_{sh}}{i_{Lh}} = \frac{1}{1+G_c(s).G_{inv}(s).G_{out}(s)} \quad (8)$$

PROPOSED CONTROL METHOD FOR HAPF

The proposed control method for HAPF is shown in Figure 5.

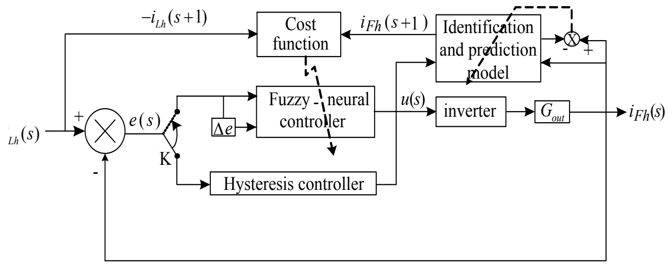

Figure 5. Proposed control method for HAPF

There are two control modes in the proposed control scheme are Hysteresis and Adaptive Fuzzy-Neural control modes. The selecting between two modes is decided by a switch K. The principle of switching as follows:

$$|e(s)| = \begin{cases} > threshold\ value \Rightarrow Hysteresis\, controller \\ \leq threshold\ value \Rightarrow Adaptive\ fuzzy-neural\, controller \end{cases}$$

Hysteresis controller :

The hysteresis control principle can be described as follows:

$$u = \begin{cases} -U & if\ e(s) < V_L \\ 0 & if\ V_L \leq e(s) \leq V_H \\ U & if\ e(s) > V_H \end{cases}$$

Where: U is a constant output, V_L is the lower bound and V_H is the upper bound.

Identification and prediction model :

The identification and prediction model is used to identify the value $I_{Fh}(s)$ and predict an output value $I_{Fh}(s+1)$. The identification and prediction model used here is a neural network with a time-delayed structure and presented as in Figure 6. The prediction error between the $I_{Fh}(s)$ and the neural network output is used as the neural network training signal.

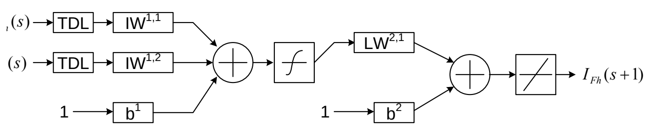

Figure 6. Neural network structure

The predictive control method is based on the receding horizon technique [15].The neural network model predicts the plant response over a specified time horizon. The predictions are used by a numerical optimization program to determine the control signal that minimizes the following performance criterion over the specified horizon

$$M=\frac{1}{2}\sum_{j=N_1}^{N_2}(-I_{Lh}(s+j)-\tilde{I}_{Fh}(s+j))^2+\frac{1}{2}\sum_{j=1}^{N_u}\lambda\left[\Delta u(s+p-1)\right]^2 \quad (9)$$

where N_1, N_2, and N_u define the horizons over which the tracking error and the control increments are evaluated. The $\Delta u(.)$ variable is the tentative control signal, $-I_{Lh}(s+j)$ is the desired response, and $\tilde{I}_{Fh}(s+j)$ is the network model response. The λ value determines the contribution that the sum of the squares of the control increments has on the performance index.

Fuzzy-neural controller:

The fuzzy-neural controller is structured by four layers [13]: input layer, fuzzy layer, rule layer and output layer.

+ Nodes at *input layer*

$$\begin{cases} O_1^1 = e.\omega_{1i}, & i=1,2 \\ O_2^1 = \Delta e.\omega_{1i}, & i=1,2 \end{cases} \quad (10)$$

where ω_{1i} is connecting weights

+ Nodes at fuzzy layer

$$O_{ij}^{fuzzylayer}=\mu_{Ai}^{j}=\exp\left(-\frac{\left(O_i^1-c_{ij}\right)^2}{2\sigma_{ij}^2}\right);\ i=1,2\ ;\ j=1,2,...7 \quad (11)$$

where c: mean, δ: standard deviation and δ^2: variance

+Nodes at rules layer.

$$O_k^{ruleslayer}=\prod_{i=1}^{2}\mu_{Ai}^{j}\ ,\ i=1,2\ ;\ j=1,2,...7;\ k=1,2,...,49. \quad (12)$$

+ The neural network layer.

$$O_{neuralnetwork}=u=\frac{\sum_{k=1}^{m}O_k^{ruleslayer}\omega_{4k}}{\sum_{k=1}^{m}O_k^{ruleslayer}}\ ;m=49 \quad (13)$$

Where: ω_{4k} is connecting weights

To update the parameters of the fuzzy neural controller, the cost function J is defined as follows:

$$J=\frac{1}{2}\sum_{i=1}^{n}\left(-i_{Lh}(s+1)-\tilde{i}_{Fh}(s+1)\right)^2 \quad (14)$$

where n is a learning sample number, $-i_{Lh}(s+1)$ is a reference value, $\tilde{i}_{Fh}(s+1)$ is the predicted output value from identification and prediction model. In order to achieve the aim of control, the back - propagation method is used to update parameters as follows:

$$\begin{cases} \omega_{4k}(s+1)=\omega(s)-\eta_k\dfrac{\partial J}{\partial\omega_{4k}}+\alpha[\omega(s)-\omega(s-1)] \\ c_{ij}(s+1)=c_{ij}(s)-\eta_k\dfrac{\partial J}{\partial c_{ij}}+\alpha[c_{ij}(s)-c_{ij}(s-1)] \\ \sigma_{ij}(s+1)=\sigma_{ij}(s)-\eta_k\dfrac{\partial J}{\partial\sigma_{ij}}+\alpha[\sigma_{ij}(s)-\sigma_{ij}(s-1)] \end{cases} \quad (15)$$

Where α is a smoothness factor, $0<\alpha<1$. η_k is a learning rate, $\eta_k>0$

The differential coefficients $\dfrac{\partial J}{\partial\omega_{4k}},\dfrac{\partial J}{\partial c_{ij}}$ and $\dfrac{\partial J}{\partial\sigma_{ij}}$ are calculated as follows

$$\frac{\partial J}{\partial\omega_{4k}}=-\left(-I_{Lh}(s+1)-\tilde{I}_{Fh}(s+1)\right)f'(O_k^{rulelayer}).O_k^{rulelayer}=\delta_k^4.O_k^{rulelayer} \quad (16)$$

With $\delta_k^4=-(-i_{Lh}-\tilde{i}_{Fh})f'(O_k^{rulelayer})$

Similarly, we have

$$\begin{cases} \dfrac{\partial J}{\partial c_{ij}}=\dfrac{\partial J}{\partial O_{ij}^{fuzzylayer}}\dfrac{\partial O_{ij}^{fuzzylayer}}{\partial c_{ij}}=\delta_k^{fuzzylayer}\dfrac{(O_i^1-c_{ij})}{\sigma_{ij}^2}.O_{ij}^{fuzzylayer} \\ \dfrac{\partial J}{\partial\sigma_{ij}}=\dfrac{\partial J}{\partial O_{ij}^{fuzzylayer}}\dfrac{\partial O_{ij}^{fuzzylayer}}{\partial\sigma_{ij}}=\delta_k^{fuzzylayer}\dfrac{(O_i^1-c_{ij})^2}{\sigma_{ij}^3}.O_{ij}^{fuzzylayer} \end{cases} \quad (17)$$

STABILITY ANALYSIS OF THE PROPOSED CONTROL METHOD

The proposed control method is stable or not stable depend on the identification and prediction model. There are many methods to analyze stability, such as: small gain theorem, *Lyapunov* stability theorem, the graphical *Lyapunov* stability region analysis, etc. In this paper, the *Lyapunov* theorem is applied to the stability analysis of the proposed control method.

For the identification and prediction model, to ensure the control system operates stable, the identification process must be successful.

Equation (9) is written in vector form as

$$M(s)=\frac{1}{2}\left(Y_r(s)-Y_n(s)\right)^T\left(Y_r(s)-Y_n(s)\right)+\frac{1}{2}\lambda_k\Delta U^T(s)\Delta U(s) \quad (18)$$

Where:

$Y_r(s) = [y_r(s+1) \quad y_r(s+2) \quad y_r(s+N_2)]^T$ is the desired value at instant (s)

$Y_n(s) = [y_n(s+1) \quad y_n(s+2) \quad y_n(s+N_2)]^T$ is the predicted output value at instant (s)

$\Delta U(s) = \frac{\eta}{1+\eta\lambda_k} G^T(s)(Y_r(s) - Y_n(s))$ is the control variation at instant (s)

With $G(s) = \left[\frac{\partial y_n(s+1)}{\partial u(s)} \quad \frac{\partial y_n(s+2)}{\partial u(s)} \dots \frac{\partial y_n(s+N_2)}{\partial u(s)}\right]^T$

$$\Delta U(s) = [\Delta u(s+1) \;\; \Delta u(s+2) \dots \Delta u(s+N_u)]^T$$

$$\Delta u(s+1) = u(s+1) - u(s)$$

If we choose the Lyapunov function candidate as

$$L(s) = (Y_r(s) - Y_n(s))^T (Y_r(s) - Y_n(s)) = E^T(s).E(s) \quad (19)$$

Where $E(s) = [e(s+1) \;\; e(s+2) \dots e(s+N_2)]^T$ and $e(s+1) = y_r(s+1) - y_n(s+1)$

The first necessary condition of Lyapunov for the stable system is $L(s) > 0$ which is apparent.

The second necessary condition for the stable system is $\Delta L \le 0$

$$\Delta L(s) = L(s+1) - L(s) = 2\Delta E^T(s)E(s) + \Delta E^T(s)\Delta E(s) \quad (20)$$

$$\Delta E(s) = -\frac{\partial Y_n(s)}{\partial u(s)} \Delta U(s) = -G(s).\Delta U(s) \quad (21)$$

$$\Delta U(s) = \frac{\eta}{1+\eta\lambda_k} G^T(s).E(s) \quad (22)$$

Substituting (21), (22) into (20), we have

$$\Delta L(s) = -\frac{\eta}{1+\eta\lambda_k} G^T(s)G(s)E^T(s)\left(2I - \frac{\eta}{1+\eta\lambda_k} G(s)G^T(s)\right)E(s) \quad (23)$$

I: is unity matrix

In order to satisfy the $\Delta L \le 0$ then

$$\frac{\eta}{1+\eta\lambda_k} G^T(s)G(s)E^T(s)\left(2I - \frac{\eta}{1+\eta\lambda_k} G(s)G^T(s)\right)E(s) \ge 0$$

Hence $\eta \le \frac{2}{G^T(s)G(s) - 2\lambda}$

Therefore, to ensure the identification process will be successful, let η>0 be an optimal rate for the neural network predictive controller and α_{max} be defined as $\alpha_{max} = \max G(s)$. Then, the convergence is guaranteed if η is chosen to satisfy

$$0 < \eta \le \frac{2}{\alpha^T{}_{max}.\alpha_{max} - 2\lambda} \quad (24)$$

Therefore, with η chosen such as in (24), then the proposed control method ensures stability.

SIMULATION RESULTS

To demonstrate effectiveness and robustness of the proposed control method, the simulation results are implemented on the HAPF model (380V-50Hz) in three cases: parameters of system are unchanged, parameters of system are changed and grid voltage is unbalance. The HAPF parameters are given in Table 1.

Table 1: HAPF parameters

L_0 (mH)	C_0 (μF)	L_1 (mH)	C_1 (μF)	C_F (μF)	V_{dc} (V)	N_1	N_2	N_u	λ
1.0	60	29.77	349.2	100	535	1.0	7.0	2.0	0.05

THD of i_L (=THD of i_s) before compensation is shown as in Figure 7. Figure 8 shows simulation results when the system parameters are unchanged. Figure 9 shows simulation results when the system parameters L_0, C_0, L_1, C_1 and C_F are changed (we assumed that the change of system parameters is limited to ± 20% of the initial values). Figure 10 shows simulation results when the grid voltage is unblance, the voltage amplitude of the phase A is increased to 10% compared to the phase B and C. Where $U_{s\text{-}abc}(V)$, $I_{L\text{-}abc}(A)$, $I_{s\text{-}abc}(A)$, $I_{Fh\text{-}abc}(A)$ and *error-abc(A)* are the three-phase source voltage, three-phase load current, three-phase supply current, three-phase compensation current and three-phase compensation error, respectively.

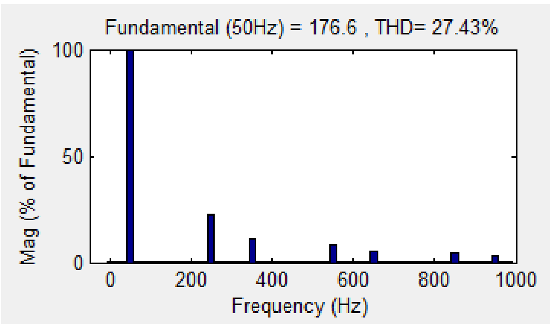

Figure 7. THD of i_L

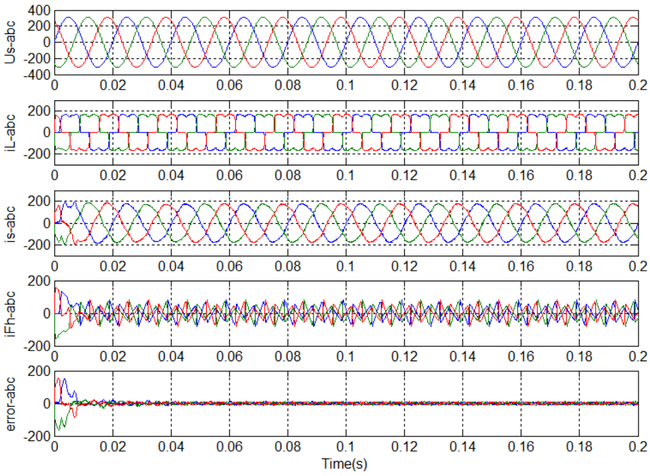

a) Simulation results with the Hysteresis controller

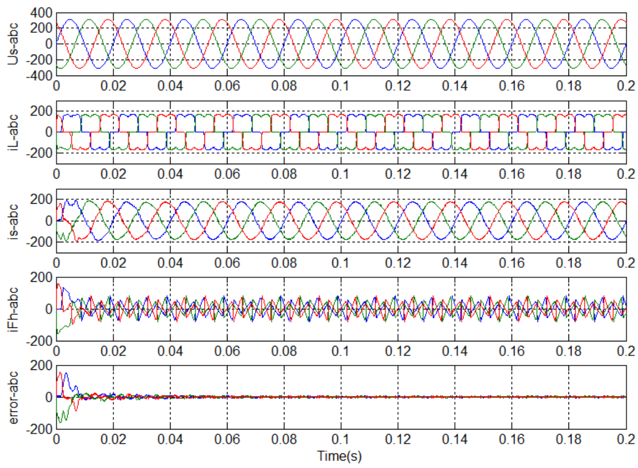

b) Simulation results with the Fuzzy-neural controller

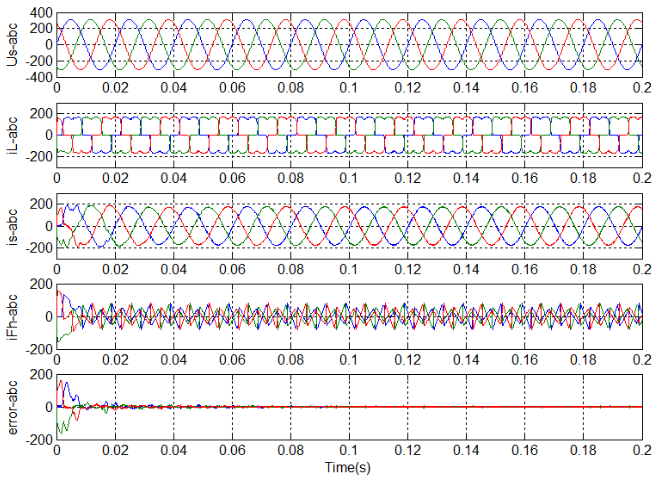

c) Simulation results with the proposed controller

Figure 8. Simulation results when the system parameters are unchanged.

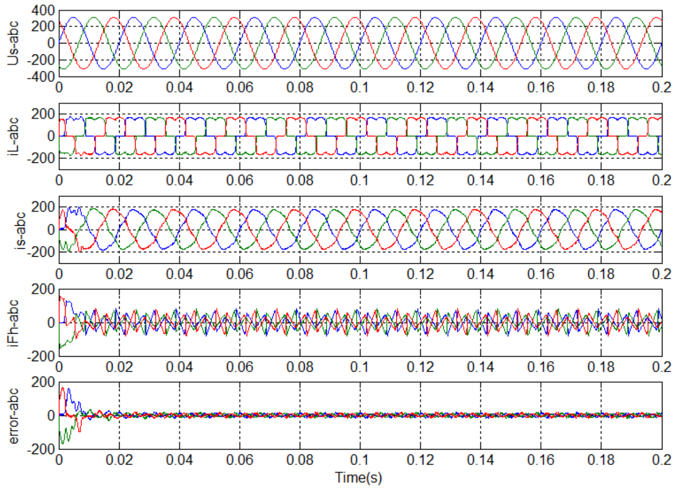

a) Simulation results with the Hysteresis controller

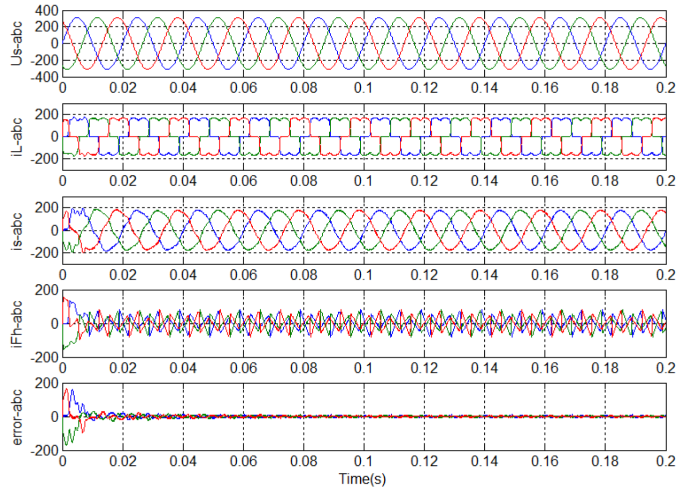

b) Simulation results with the Fuzzy-neural controller

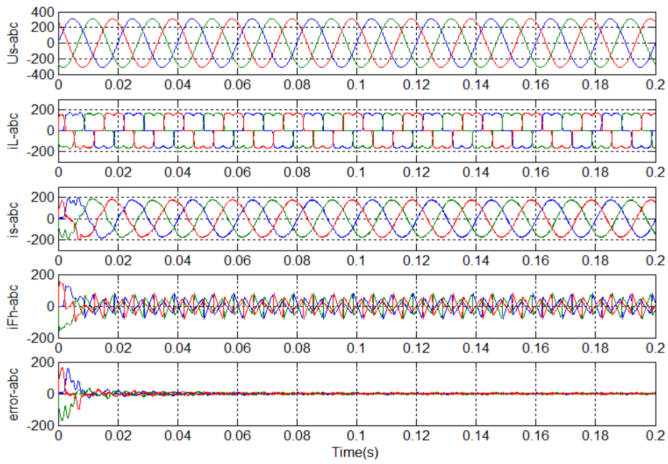

c) Simulation results with the proposed controller

Figure 9. Simulation results when the system parameters are changed.

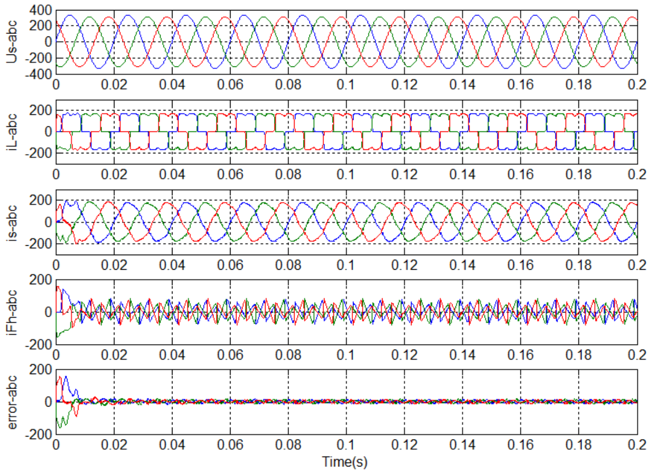

a) Simulation results with the Hysteresis controller

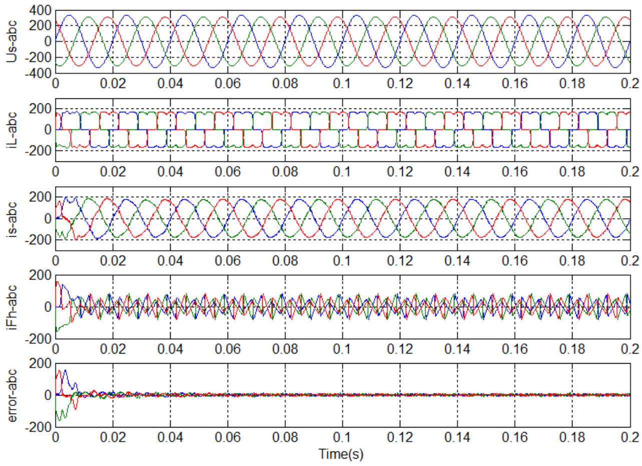

b) Simulation results with the Fuzzy-neural controller

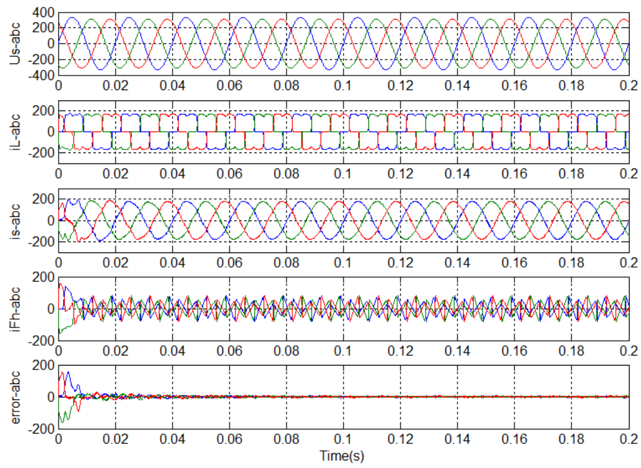

c) Simulation results with the proposed controller

Figure 10. Simulation results when the grid voltage is unbalance.

From the simulation results in Fig.8, Fig. 9 and Fig. 10, we can see that:

When the system parameters are unchanged: with the Hysteresis controller is used, the compensation error is reduced to ±15A from ±80A in 0.0s-0.04s and this error is constant until 0.2s. With the Fuzzy neural controller is used, the compensation error is reduced to ±12A from ±80A in 0.0s-0.04s and then reduced to ±8A in 0.19s-0.2s. With the proposed controller is used, the compensation error is reduced to ±10A from ±80A in 0.0s-0.04s and then reduced to ±4A in 0.19s-0.2s.

When the system parameters are changed (limited to ± 20% of the initial values). With the Hysteresis controller is used, the compensation error is reduced to ±25A from ±80A in 0.0s-0.04s and this error is constant until 0.2s. With the Fuzzy neural controller is used, the compensation error is reduced to ±15A from ±80A in 0.0s-0.04s and then reduced to ±10A in 0.19s-0.2s. With the proposed controller is used, the compensation error is reduced to ±10A from ±80A in 0.0s-0.04s and then reduced to ±5A in 0.19s-0.2s.

When the grid voltage is unbalance, the voltage amplitude of the phase A is increased to 10% compared to the phase B and C. With the Hysteresis controller is used, the compensation error is reduced to ±20A from ±80A in 0.0s-0.04s and this error is constant until 0.2s. With the Fuzzy neural controller is used, the compensation error is reduced to ±15A from ±80A in 0.0s-0.04s and then reduced to ±8A in 0.19s-0.2s. With the proposed controller is used, the compensation error is reduced to ±12A from ±80A in 0.0s-0.04s and then reduced to ±5A in 0.19s-0.2s.

THD of the supply current with the difference cases is summarized as in table 2.

Table 2: THD of the supply current with the difference cases

	THD i_s %		
Cases	**Hysteresis controller**	**Fuzzy neural controller**	**Proposed controller**
System parameters are unchanged	4.13	2.22	1.3
System parameters are changed	6.19	2.96	1.99
Grid voltage is unbalance	5.41	2.92	1.69

From the above analysis results, we can see that the proposed controller has a better dynamic response time than, better steady-state performance than compared with Hysteresis and Fuzzy-neural controllers. Moreover, ability to cancel harmonics is very effective and especially the ability to adapt to the changes of the system is very well.

CONCLUSION

This paper was proposed a new control method for HAPF. Compared with the methods using Hysteresis and Fuzzy-neural network controllers, the proposed control method shown many advantages such as decrease in the tracking error, decrease in dynamic response time, harmonics eliminative capability is very effective. Moreover, the ability to adapt with the system variance is very well. Simulation results have demonstrated the effectiveness and robustness of the proposed controller.

REFERENCES

[1] Ertay, M, M., Tosun S., and Zengin, A., 2012, "Simulated annealing based passive power filter design for a medium voltage power system", International Symposium on Innovations in Intelligent Systems and Applications (INISTA) , pp. 1-5.

[2] Junpeng Ji., Guang Zeng., Haiwa Liu., Lei Luo and Jinggang Zhang., 2012, "Research on selection method of Passive Power Filter topologies", 7th International Power Electronics and Motion Control Conference (IPEMC), pp. 2844-2848.

[3] Ge J J., Zhao Z M., and Li J J., 2013, "Backstepping control for active power filter with LCL filter", 2nd IET Renewable Power Generation Conference (RPG), pp. 1-4.

[4] El Habrouk M., Darwish M K., and Mehta P., 2000, "Active Power Filters," IEE Electric Power Applications., 147(5), pp. 403-413.

[5] N Mohan., H A Peterson., W F Long., G R Dreifuerst., and J Vithayathil., 1977, "Active filters for AC harmonic suppression," in IEEE power Eng. Soc. Winter Meeting, pp. 657-663.

[6] H Fujita., and H Akagi., 1991, "A practical approach to harmonic compensation in power system-series connection of passive and active filters," IEEE Transactions on Industry Applications., 27(6), pp. 1020-1025.

[7] F Ruixiang., L An., and L Xinran., 2006, "Parameter design and application research of shunt hybrid active power filter," Proc. CSEE., 26(2), pp. 106-111.

[8] Liu Wei., and Zhang Dawei., 2012, "Study on a series hybrid active power filter based on novel fuzzy immune PID controller," International Conference on Measurement, Information and Control (MIC), pp. 520-523.

[9] Suresh Y., Panda A K., and Suresh M., 2012, "Real-time implementation of adaptive fuzzy hysteresis-band current control technique for shunt active power filter," IET Power Electronics., 5(7), pp. 1188-1195.

[10] An Luo., Zhikang Shuai., Wenji Zhu., Ruixiang Fan., and Chunming Tu., 2009, "Development of Hybrid Active Power Filter Based on the Adaptive Fuzzy Dividing Frequency-Control Method," IEEE transactions on power delivery., 24(1), pp. 424-432.

[11] Chen Wei., LI Qin., Lu Tingjin., Rong Penghui., and Zhao Yanqing., 2010, "Method of Event Detection Based on Dynamic Hybrid Fuzzy Logic System," in International Conference on Intelligent Computation Technology and Automation, pp. 661-663.

[12] Ahmed A Helal., Nahla E Zakzouk., and Yasser G Desouky., 2009, "Fuzzy Logic Controller Shunt Active Power Filter for Three-phase Four-wire systems with Balanced and Unbalanced Loads," World Academy of Science, Engineering and Technology., 58(2), pp. 621-626.

[13] Yih-Guang Leu., Tsu-Tian Lee., and Wei-Yen Wang., 1997, "On-Line Tuning of Fuzzy–Neural Network for Adaptive Control of Nonlinear Dynamical Systems," IEEE Transactions On Systems, Man, And Cybernetics., 27(6), pp. 1034-1043.

[14] J Mazumdar., R G Harley., and F C Lambert., 2007, "Neural network based method for predicting nonlinear load harmonics," IEEE Trans. Power Electron., 22(3), pp. 1036-1045.

[15] Soloway D., and P.J.Haley., 1996, "Neural Generalized Predictive Control," Proceedings of the IEEE International Symposium on Intelligent Control, pp. 277-281.

[16] Rodriguez J., Pontt J., Silva C A., Correa P., Lezana P., Cortes P., and Ammann U., 2007, "Predictive current control of a voltage source inverter," IEEE Transactions on Industrial Electronics., 54(1), pp. 495-503.

[17] Ghazanfarpour B., Radzi M A M., Mariun N., and Shoorangiz R., 2013, "Adaptive unified neural network for dynamic power quality compensation," IEEE 7th International Power Engineering and Optimization Conference (PEOCO), pp. 114-118.

[18] Kumar A S., and Raj P A., 2011, "Neural learning algorithm based power quality enhancement for three phase three wire distribution system utilizing shunt active power filter strategy," International Conference on Power and Energy Systems (ICPS), pp. 1-6.

[19] Fei Juntao., Wang Zhe., Lu Xiaochun., and Deng Lihua., 2013, "Adaptive RBF neural network control based on sliding mode controller for active power filter," 32nd Chinese Control Conference (CCC), pp. 3288-3293.

[20] Wang Xiaogang., Xie Yunxiang., Shuai Dingxin., 2008, "Simplified model predictive control for a shunt active power filter," Conference in Power Electronics Specialists, pp. 3279-3283.